AD-A044 655 SOUTHWEST RESEARCH INST SAN ANTONIO TEX F/G 11/2
COMPRESSIVE MICROFRACTURE AND INDENTATION DAMAGE IN AL203.(U)
AUG 77 J LANKFORD N00014-75-C-0668
UNCLASSIFIED SWRI-02-4231-001 NL

1 OF 1
ADA
044655

END
DATE
FILMED
10-77
DDC

(12)

COMPRESSIVE MICROFRACTURE AND INDENTATION DAMAGE IN ALUMINA

by
James Lankford, Jr.

TECHNICAL REPORT

ONR Contract No. N00014-75-C-0668
ONR Contract Authority NR 032-553/1-3-75(471)
SwRI Project No. 02-4231

for
Office of Naval Research
Arlington, Virginia 22217

by
Southwest Research Institute
San Antonio, Texas

August 30, 1977

SOUTHWEST RESEARCH INSTITUTE
SAN ANTONIO CORPUS CHRISTI HOUSTON

Unclassified

SECURITY CLASSIFICATION OF THIS PAGE (When Data Entered)

REPORT DOCUMENTATION PAGE

READ INSTRUCTIONS BEFORE COMPLETING FORM

1. REPORT NUMBER	2. GOVT ACCESSION NO. / 3. RECIPIENT'S CATALOG NUMBER
4. TITLE (and Subtitle): Compressive Microfracture and Indentation Damage in Al_2O_3	5. TYPE OF REPORT & PERIOD COVERED: Interim Technical Report. 1 Mar 77 — 30 Aug 77.
	6. PERFORMING ORG. REPORT NUMBER: 02-4231-001
7. AUTHOR(s): James Lankford, Jr.	8. CONTRACT OR GRANT NUMBER(s): N00014-75-C-0668
9. PERFORMING ORGANIZATION NAME AND ADDRESS: Southwest Research Institute, P. O. Drawer 28510, San Antonio, Texas 78284	10. PROGRAM ELEMENT, PROJECT, TASK AREA & WORK UNIT NUMBERS: NR 032-553/~~1-3-75(471)~~
11. CONTROLLING OFFICE NAME AND ADDRESS: Office of Naval Research, 800 North Quincy, Arlington, Virginia 22217	12. REPORT DATE: 30 Aug 77
	13. NUMBER OF PAGES: 196
14. MONITORING AGENCY NAME & ADDRESS (if different from Controlling Office)	15. SECURITY CLASS. (of this report): Unclassified
	15a. DECLASSIFICATION/DOWNGRADING SCHEDULE

16. DISTRIBUTION STATEMENT (of this Report)

Distribution is unlimited.

DISTRIBUTION STATEMENT A
Approved for public release;
Distribution Unlimited

17. DISTRIBUTION STATEMENT (of the abstract entered in Block 20, if different from Report)

18. SUPPLEMENTARY NOTES

19. KEY WORDS (Continue on reverse side if necessary and identify by block number)

Microplasticity	Thermal Activation
Indentation	Acoustic Emission
Twinning	Microcrack Initiation
Compression	Fracture Mode

20. ABSTRACT (Continue on reverse side if necessary and identify by block number)

Compressive damage in alumina has been characterized as a function of strain rate and temperature. Scanning electron microscopy and acoustic emission were employed in examining both the early crack initiation and later failure stages of damage caused by uniaxial compressive stress. The formation of lateral cracks produced during indentation loading is characterized in terms of microplasticity, and the particle velocity range over which the mechanism is expected to be operative is computed.

DD FORM 1 JAN 73 1473 EDITION OF 1 NOV 65 IS OBSOLETE

328 200

Unclassified

SECURITY CLASSIFICATION OF THIS PAGE (When Data Entered)

FOREWORD

This report describes the results of experiments carried out during a program directed toward assessing the role of compressive stresses and compression-induced damage in the failure of a brittle ceramic. The temperature and strain rate dependence of both early microcrack formation and ultimate failure under uniaxial compressive loading are described, and indentation microcracking is considered in terms of compressive damage mechanisms.

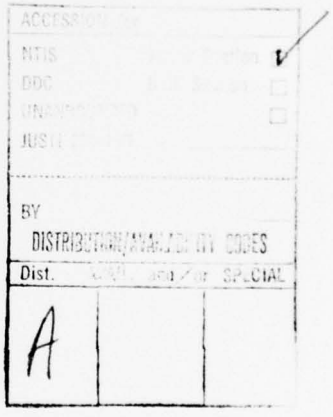

COMPRESSIVE MICROFRACTURE AND INDENTATION DAMAGE IN Al_2O_3

During the impact of ceramics by small hard particles, indentation damage is caused, which can lead to erosion and/or strength degradation of the ceramic. It is suspected that certain types of indentation-induced flaws may be generated by the compressive fields known to be associated with such loading. Accordingly, a research program was carried out to assess the mechanisms of damage in a strong ceramic subject to compressive loading, and to determine, if possible, the relevance of such mechanisms to indentation damage.

Initial results, indicating that the early stages of compressive damage in Al_2O_3 consist of twinning and twin-induced microcracking, have been reported.[1] In addition, it was shown that the compressive strength was strain rate sensitive. In the present report the earlier results are extended over wider ranges in temperature and strain rate, and interpreted through acoustic emission experiments designed to detect the onset of microplasticity. Furthermore, the temperature dependence of the fractography associated with ultimate failure is characterized using scanning electron microscopy. The results of an SEM study of indentation in the same material are also reported, and it is shown that compressive damage in the form of twinning is important in nucleating the lateral microcracks thought[2,3] to be responsible for erosion. Based on the compressive test-acoustic emission data, the particle velocity regime over which the twin/microcrack erosion mechanism seems relevant is estimated.

EXPERIMENTAL PROCEDURES

The compression test set-up and procedures have been described in detail elsewhere,[1] and are discussed here only briefly. Compression specimens were fabricated in the form of right circular cylindrical specimens cut from as-received rods of polycrystalline Lucalox* alumina, having a 25μm grain size. The ends of the 1.25 cm long x 0.625 cm dia. specimens were ground parallel and polished to a mirror finish. Compression tests were carried out using platens of Coors AD 999 alumina.† Strain rates ranged from 7×10^{-6} sec^{-1} to 2×10^{3} sec^{-1}, with the latter rates being achieved by means of the Hopkinson pressure bar; temperatures were varied from -200° to 900°C. Not all tests were carried out to failure; in particular, certain specimens were loaded to predetermined levels, during which loading period acoustic emission was monitored, and then unloaded and coated with palladium for study in the SEM to detect any damage which might have been incurred. The fracture surfaces of failed specimens also were examined in the SEM.

Acoustic emission (AE) was monitored during certain compression tests within the frequency domain 100 kHz to 1 MHz, with a transducer resonance of 160 kHz. The signal was passed through an 80 dB gain amplifier, a filter, and an adjustable discriminator, whose level, once set, remained constant

*Type GW, General Electric Lamp Glass Division, Cleveland, Ohio.
†Coors Porcelain Company, Golden, Colorado

for all tests. Pulses from the discriminator entered a 5-decade counter and a digital waveform recorder together with the compressive stress/time signal. Following the test, the recorder was played back through a strip-chart recorder to yield as function of time both stress and accumulated counts. The best fit curve to the latter was differentiated and plotted versus the former to provide the count rate as a function of stress. This method of treating the AE information is similar to that used by others[4,5] studying the tensile strength of ceramics.

In addition to the compressive strength tests, some of the as-fired rods were indented statically with a diamond pyramid micro-hardness indenter. Individual grains were selected for multiple indentation at sequentially higher loads, with indenter orientation maintained constant within a given grain. For comparison, the polished surface of a large [0110] oriented, sapphire single crystal was indented in the same way. Following indentation, the specimens were coated and examined in the scanning electron microscope.

RESULTS

Compressive Strength

The compressive strength of σ_f of Lucalox as a function of temperature T behaves in a manner reminiscent of its tensile strength. As shown in Figure 1, the strength, for two different strain rates ($\dot{\varepsilon}$), decreases with increasing temperature, then rather suddenly begins to increase, before finally settling back into an inverse relationship with temperature. Bend tests performed on the same material[6] in air and vacuum exhibit qualitatively the same behavior, except that the average strength is lower by an order of magnitude, and the strength minimum occurs at around 350°C rather than 150° to 250°C. Extrapolating the lower strain rate data to absolute zero yields a projected ultimate compressive strength of about 4200 MN/m^2.

The thermally activated nature of the compressive failure process is further exemplified by the dependence of strength upon strain rate, plotted in Figure 2. Over nine orders of magnitude in strain rate, the strength experiences approximately a 45% increase. However, it would appear, based on the ultimate strength of 4200 MN/m^2 derived from the σ_f-$\dot{\varepsilon}$ data, that the effect should persist to strain rates in excess of 10^8 sec^{-1}.

The resemblance between the σ_f-T curves for tension and compression is reflected in the fracture surface appearance as well. As shown in Figure 3, low temperature tests exhibit mixed-mode fracture surfaces, i.e., combined intergranular and transgranular. At liquid nitrogen temperatures, both modes are present in roughly equal proportion, but with increasing temperature, the propensity for intergranular failure increases(Figure 4). Around 900°C, failure is almost totally intergranualar, except for certain regions (arrows, Figure 5) which appear to have failed by transgranular cleavage along multiple crystallographic planes. Such a region is shown at higher magnification in Figure 6.

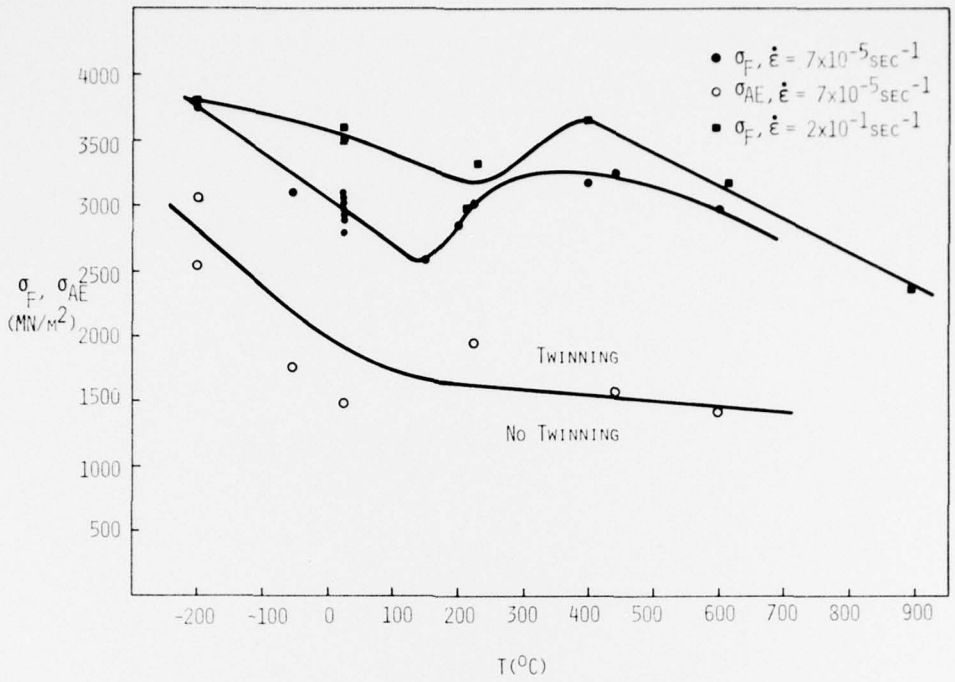

Figure 1. Compressive Strength and Threshold Stress Level for Acoustic Emission Versus Temperature

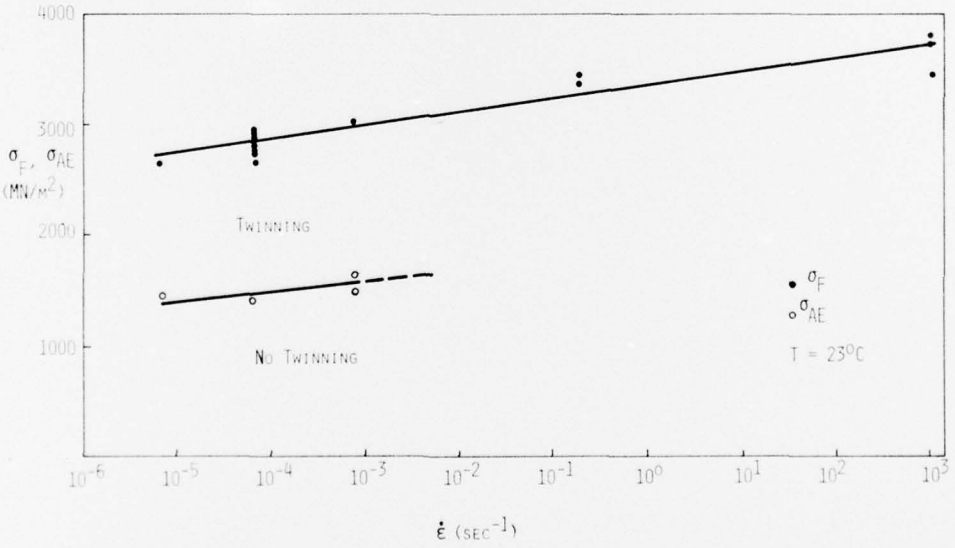

Figure 2. Compressive Strength and Threshold Stress Level for Acoustic Emission Versus Strain Rate

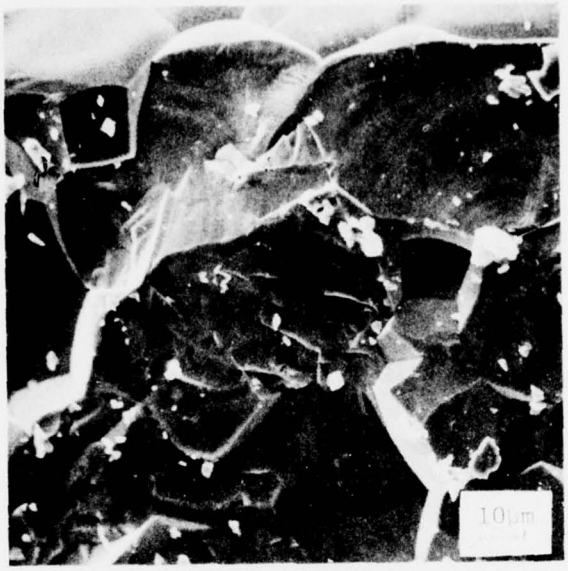

Figure 3. Compressive Fracture Surface, T = -200°C

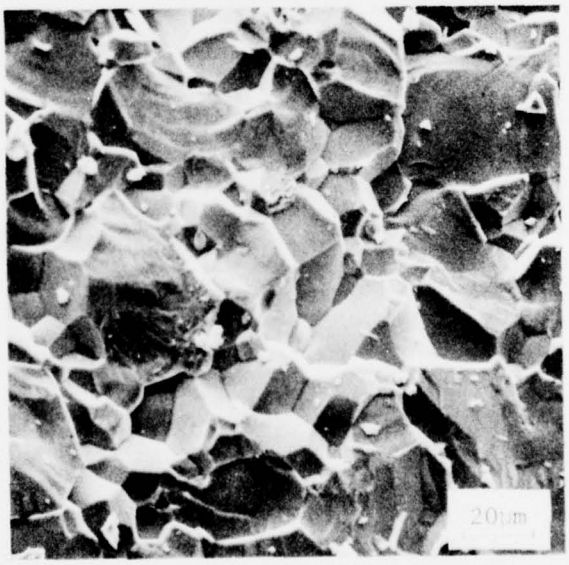

Figure 4. Compressive Fracture Surface, T = 443°C

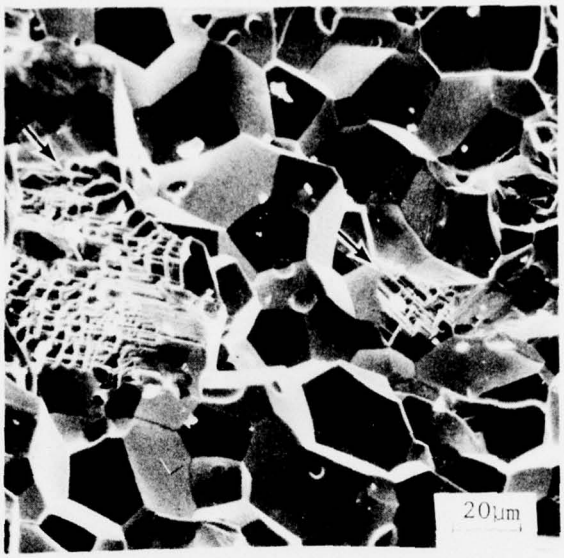

Figure 5. Compressive Fracture Surface, T = 892°C

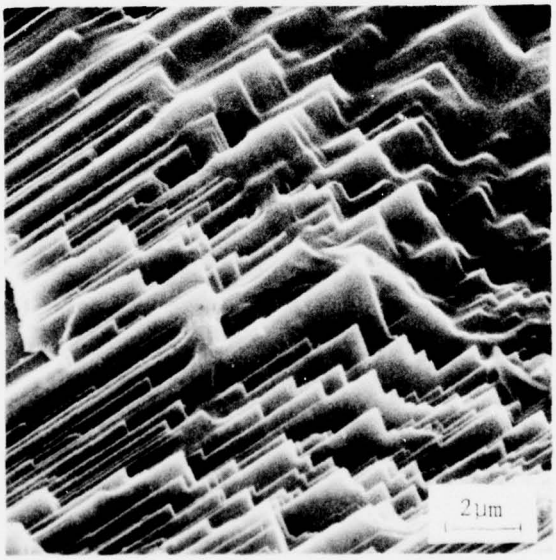

Figure 6. Details of Faceted Transgranular Fracture, T = 892°C

Acoustic Emission

The onset of acoustic emission due to damage (σ_{AE}) is defined as the stress level at which the acoustic emission count rate first begins to exceed the background rate, usually a few counts per second, determined by the discriminator level. In Figures 1 and 2, σ_{AE} is plotted as a function of temperature and strain rate, respectively. It is apparent that damage begins at stress levels well below that required to cause fracture. The curve for acoustic emission stress level parallels that for failure strength from -200 to around 200°C in Figure 1, but does not reflect the subsequent increase in strength. Similarly, the σ_{AE}-$\dot{\varepsilon}$ data plotted in Figure 2 follow the σ_f-$\dot{\varepsilon}$ reasonably well over the limited range in $\dot{\varepsilon}$ within which AE was obtained. This would be expected from the σ_{AE}-T results, i.e., as was the case with decreasing T, the strength increases with $\dot{\varepsilon}$ from that at $\dot{\varepsilon} \sim 10^{-4}$ sec^{-1}, T = 23°C. The strain rate range for AE was limited to that shown in Figure 2 by the fact that at higher strain rates, the transducer was forced to count at rates in excess of its capability to respond.

As in the case of σ_f, an extrapolation to absolute zero may be carried out for σ_{AE}, yielding (Figure 1) an ultimate stress for twinning of $\sim$ 3100 MN/m^2. Extrapolation of the σ_{AE}-$\dot{\varepsilon}$ data in Figure 2 to this stress level would imply the requirement of a strain rate in excess of 10^8 sec^{-1} in order to suppress twinning at room temperature.

SEM study of specimens loaded to various stress levels showed that below the threshold stress level for acoustic emission, no damage was discernible. Above this level, twinning was visible in many grains, and as stress levels were increased, still more twins were produced, and microcracks began to appear, associated with twin-grain boundary intersections and with twin plane decohesion. This aspect of compressive strength, i.e., the role of twinning in causing microcracking in Lucalox, has recently been documented extensively by the writer.[1] In the present context, the main point is that the thermally activated mechanism detected by the AE is deformation twinning. In addition, as documented in an earlier study[7] of tensile failure, twins formed above 200°C were generally thicker than those nucleated at lower temperatures, and there was a greater tendency for twins to themselves nucleate additional twins in adjacent grains.

In addition to these general observations, recent study of higher temperature specimens has revealed certain apparently microplastic features which may shed light concerning fracture mechanisms. From -200°C to 400°C, the only evidence of microplasticity seems to be twins, such as are shown in Figure 7. However, at 600°C, rather wavy, slip-like features have been observed, sometimes associated with transgranular microfracture, as in Figure 8 (arrows). The waviness of these marking contrasts with the extremely sharp, planar appearance of the twins (Figure 7). High magnification study of specimens stressed at 892°C also reveals the presence of these wavy surface markings (Figure 9).

At the same temperature, an additional defect mechanism is observed.

Figure 7. Twinning, T = -200°C

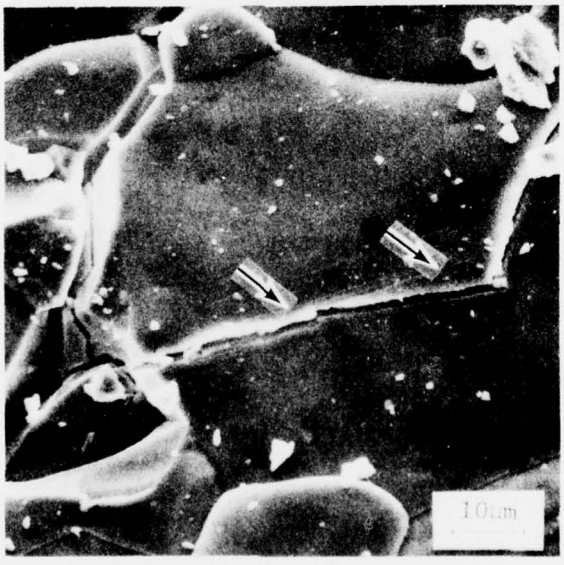

Figure 8. Mixed Intergranular and Transgranular Fracture, T = 598°C (Arrow shows wavy slip associated with transgranular crack)

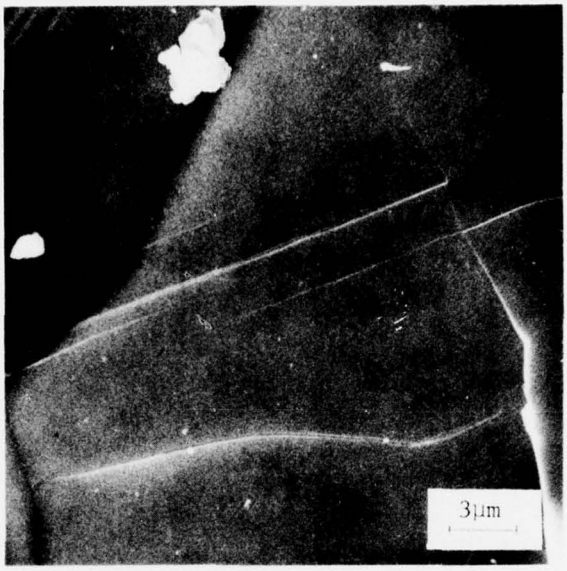

Figure 9. Wavy Slip, T = 892°C

These features have the form, as shown in Figures 10 and 11, of what appear to be serrated twins. Study of the serrations, Figure 12, shows that they are crystallographic, and that the serrations have rotated or sheared out of the grain. In Figure 12, the relationship between the serration edges and the thermally etched crystallographic planes is unmistakable. It appears that these regions constitute transgranular fractures which would have a serrated or faceted cross section.

Indentation Testing

In this section, the sequence of events corresponding to the early stages of indentation damage in Al_2O_3 are examined in greater detail than heretofore reported.[8] As shown in Figure 13a, the first evidence of damage in the polycrystalline material loaded to 5 gm is the indent, plus faint surface deformation markings (arrow) near one edge. At higher loads within the same grain, precisely the same pattern occurs, but the larger indentation now exhibits radial cracking, and the surface markings are more distinct. In Figure 13b, these features, caused by a 50 gm load, are clearly evident, as are additional faint markings along the walls of the indent (arrow); the intense surface markings are in the same location as those first appearing at 5 gm. It is interesting to note that the lower radial crack (R) is standing open, and that it seems to end near the apex of the indent.

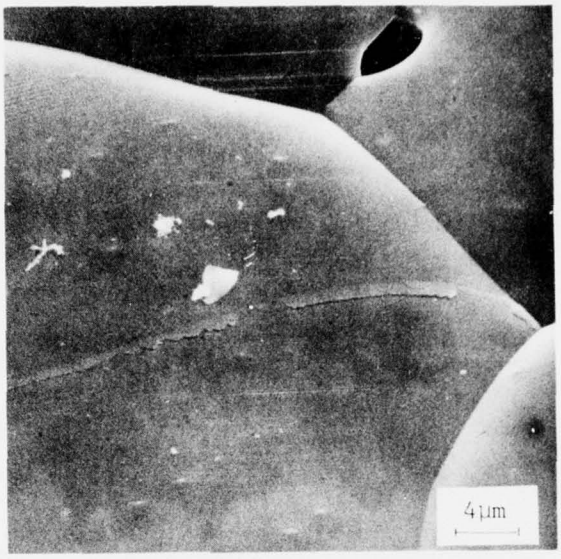

Figure 10. Serrated Microfracture, T = 892°C

Figure 11. Serrated Microfracture, T = 892°C

Figure 12. Details of Serrated Microfracture, Showing Crystallographic Dependence

In another grain (Figure 13c), indentation at 100 gm has produced deformation bands which appear to be twins, based on their resemblance to the obvious twins previously observed in compression tests.[1] Here the twins are continuous from the interior of the indent out onto the specimen surface. At the locations indicated by the arrows, the twins have begun to crack along their habit planes. Such sites appear to be the nuclei for lateral crack formation, as shown in Figure 13d; note the twins (arrow) running along the base of the lateral crack (L) in the lower portion of the photomicrograph.

At 400 gm, lateral cracking produces chipping, as in Figure 14. The origin of this crack is shown in Figure 14b, lying just below the rim of the indent. The flat plane shown (arrow) probably is a twin habit plane; note the twins on the surface to the left. Behavior similar to that described for polycrystalline alumina is found in sapphire as well. In Figures 15a and 15b, loads of 200 gm and 400 gm, respectively, produce lateral cracking (L) in identical locations. Because of the angle of the specimen relative to the beam, the deformation bands responsible for nucleation of the cracks do not show up, but they resemble those indicated by the arrow in Figure 15b. In Figure 15c, a 700 gm load has caused lateral crack chipping in two quadrants. A higher magnification view (Figure 15d) shows twins (arrow) and the flat twin facet (F) which is the apparent origin of the right hand spall. Twin band cracking (C) is also evident along the lower left corner of the indent.

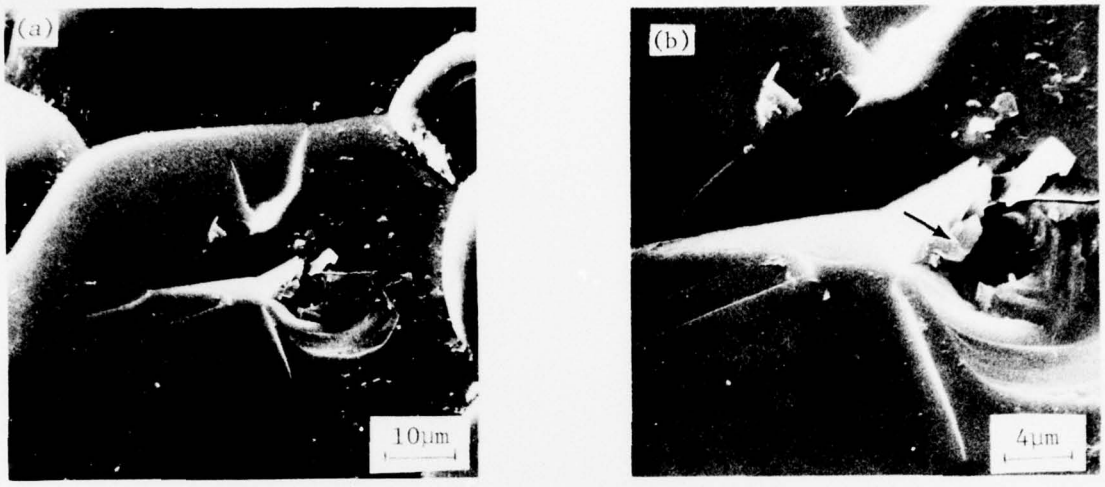

Figure 14. Indentation under 700 gm load in Lucalox (a). Chipping caused by lateral crack formation (b). Higher magnefication view, showing nucleation site (arrow).

more plentiful twins at higher temperatures. Similarly, increased strain rates inhibit twinning, hence microcrack nucleation, and thereby raise the strength.

The σ_f-T minimum is more difficult to explain. It is possible that the thickening of twins may play a role, by allowing twinned grains to accommodate greater strain without cracking. The process of thickening, a thermally activated mechanism distinct from that of initiation, would not be expected to cause detectable AE, and would agree with the observation of no change in the σ_{AE}-T curve in the region of the minimum. Alternatively, the minimum might be accounted for by the observed tendency for twins nucleated at and above[7] the σ_f-T minimum to in turn initiate twins in adjacent grains, rather than microcracks as at lower temperatures. The enhanced thermal activity in this case would serve to promote twinning on otherwise less highly active twin systems.

Based on conventional thermal activation theory, it is possible to calculate an activation energy for the twinning process, using the σ_{AE}-T and σ_{AE}-$\dot{\varepsilon}$ data. In its simplest form, the Arrhenius rate equation may be written as

$$\dot{\varepsilon} = \dot{\varepsilon}_0 \exp\left[\frac{-U(\sigma)}{RT}\right] \qquad (1)$$

where the activation energy $U(\sigma)$ is assumed to be a function of the

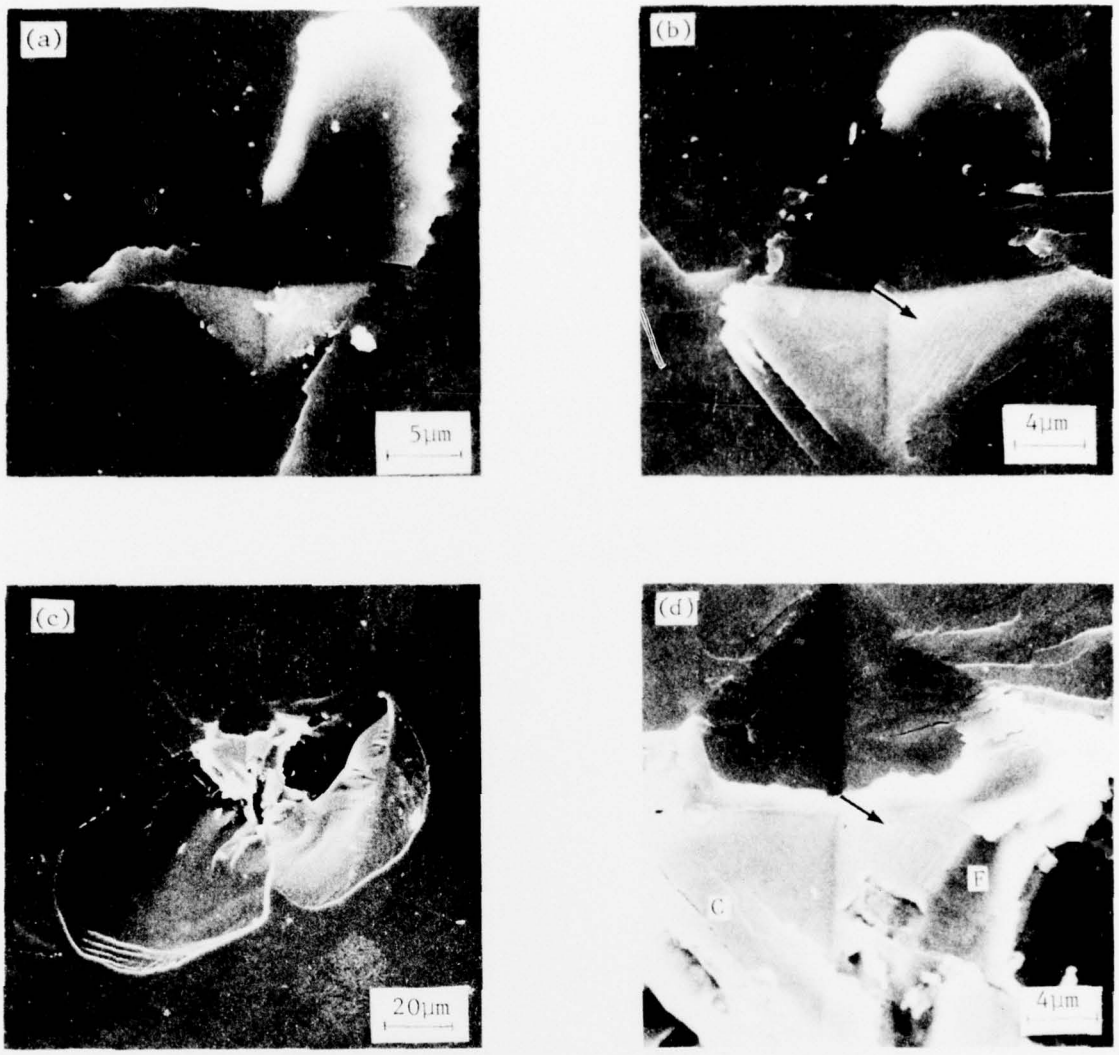

Figure 15. Indentation in sapphire (a) 200 gm load, showing lateral cracking (b) 400 gm load, showing lateral cracking as in (a), twins on indent wall (arrow) (c) 700 gm load, showing lateral crack chipping (d) Higher magnification view of (c), showing twins (arrows), twin facet (F) at lateral crack nucleation site, and twin plane cracking (c).

effective stress σ only. Here $\dot{\varepsilon}_0$ is the strain rate corresponding to the ultimate stress achieved, R is the gas constant, and T the absolute temperature. In our case, $\sigma=\sigma_{AE}$. Assuming that the stress dependence of the activation energy is linear, we can write

$$U(\sigma) = U_0 - V(\sigma_{AE} - \sigma_0) \qquad (2)$$

where U_0 is the total activation energy of the process, V is the activation volume, and σ_0 the minimum stress required to produce fracture. Substituting Equation (2) into Equation (1) yields

$$\sigma_{AE} = \frac{U_0}{V} + \sigma_0 - \frac{RT}{V} \ln \frac{\dot{\varepsilon}_0}{\dot{\varepsilon}}$$

From the data obtained in the AE experiments, $\sigma_0 \approx 1500$ MN/m^2, and $\dot{\varepsilon}_0 \approx 10^8$ sec^{-1}. On this basis, the total activation energy for twinning is estimated to be approximately 18 kcal/mole. This value is considerably lower than that determined from tests carried out at higher homologous temperatures, where dislocation mechanisms predominate. In the latter case, activation energies are on the order of 85 kcal/mole.[9] It should be noted that a valid activation energy cannot be calculated using simply the compressive strength data, since compressive failure is a composite process involving crack nucleation, growth and coalescence.[1]

The idea that the σ_f-T minimum is in some way related to the twinning process, and associated crack initiation, is compatible with the observed fractographic behavior. That is, no dramatic change in fractography is observed in the region of the minimum; rather, the fracture mode is changing slowly from mixed mode to predominantly intergranular. The same trend has been observed by a number of workers[10-12] studying the tensile fractography of alumina over the same temperature range.

Considering together the observations of the deformation markings and the failed specimen fractography, it seems reasonable to suggest the following. At lower temperatures, at least some of the transgranular fractures tend to correspond to the twin planes whose traces are visible as microplastic surface deformation. Others are caused by twin/grain boundary intersections, and the resultant initiation of axial, transgranular cracks. Above room temperature, intergranular separation is increasingly favored, possibly through limited grain boundary slip.[13] At around 900°C, plasticity through dislocation flow (as opposed to twinning alone) may extend into the grains, causing transgranular fracture through slip plane decohesion. In addition, this temperature range exhibits the apparent twinning/serrated cleavage mechanism, which seems to be so strongly crystallographic, and which probably corresponds to the relatively rare transgranular fractures, also faceted, seen at these temperatures. It is clear, incidentally, that the twins form first, followed by the facets, since both unserrated and partially serrated twins are observed in the temperature range of the mechanism.

The sharpness and clarity of the cleavage facets and intergranular separations are interesting. These characteristics would imply that no interfacial sliding sufficient to cause grooving, chipping, or other mixed-mode crack growth damage mechanisms had taken place. Moreover, since the compressive failure of Al_2O_3 is environmentally insensitive,[1] mode I cracking also is not very likely, suggesting that compressive "failure" corresponds principally to microcrack coalescence, causing the specimen, in

essence, to explode. Such a failure process would be compatible with the strong resemblence, as a function of temperature, of the compressive and tensile fractographic features.

Indentation

It seems clear that twins play a significant role in the nucleation of lateral cracks during the indentation of Lucalox. This is in qualitative agreement with speculation by several workers[2,3] that lateral crack formation, possibly as opposed to radial cracking, probably will be found to be controlled by the plastic damage zone beneath the indentation. In the present case, additional support for this idea is found in the extreme repeatability of the lateral microcracking sequence for a given indentation orientation, as exemplified by Figures 15a and 15b. Only crystallographically related crack initiators, such as twins, could reproduce the same crack morphology so consistently.

The suggestion that the specific lateral crack nucleation defects are twins in the case of Lucalox rests on several factors, primarily the observed twin/parent decohesion along indent walls, as typified in Figure 13c. In addition, this decohesion begins to occur in the same load range as does lateral cracking. Hockey[14] has pointed out that TEM studies show that whereas the bulk of the indentation plasticity in sapphire is confined below the indent, microtwins can extend up from this region to the surface of the indentation, where the lateral cracks seem to form.

It is important to consider the operational range (temperature, particle velocity) over which particulate erosion of alumina might be affected by a lateral microcrack mechanism based on twin-induced cracking. From the experimental measurements, the ultimate stress for twinning apparently corresponds to a strain rate on the order of 10^8 sec^{-1}. Assuming an indentation depth of about 5 μm, and an indentation strain of ~ 0.08,[15] an ultimate indenter velocity of around $5x10^3$ m/sec is calculated. Considering that twins propagate at sonic velocity[12], i.e., $9x10^3$ m/sec in alumina, the estimated ultimate velocity is reasonable.

Most of our information on the relationship between impact and twinning comes from studies of metals. In many of these systems, the number of twins increases with strain rate, although the twinning stress also increases.[16] Consequently, twin-nucleated microcracking in alumina might well be expected at high particle impact velocities. On the other hand, the speed of twin growth may limit the size of twins, which might in turn limit lateral microcrack extension. The latter is expected to be related to the initial flaw (twin) maximum dimension, and to the volume of stressed material. That is, extension of lateral cracks is controlled by tensile stresses originating during the unloading portion of the indentation event, and acting on the crack nucleating flaw according to fracture mechanics considerations. Crack extension in a particular stress field then requires the presence of a flaw in excess of some critical size.

Most particulate impact environments of engineering interest would involve temperatures above 23°C. Within the regime studied, i.e., 23°C to 900°C, σ_{AE} was essentially athermal. Consequently, it is most likely that over this temperature range, strain rate (particle velocity) effects would dominate crack initiation, with substrate temperature a secondary variable.

CONCLUSIONS

Compressive failure of polycrystalline aluminia is thermally activated, with an apparent basis in twin-nucleated microcracking. The latter process controls lateral crack formation, hence erosion, during indentation. It is likely that twinning and associated lateral crack formation in Al_2O_3 can persist to quite high velocities, on the order of 5×10^3 m/sec., during particulate impact.

REFERENCES

1. J. Lankford, Jour. Mat. Sci., 12, 1977, 791.
2. B. R. Lawn and M. V. Swain, Jour. Mat. Sci., 10, 1975, 113.
3. A. G. Evans and T. R. Wilshaw, Acta Met., 24, 1976, 939.
4. A. G. Evans and M. Linzer, Jour. Am. Cer. Soc., 56, 1973, 575.
5. A. G. Evans, M. Linzer, and L. R. Russell, Jour. Mat. Sci., 15, 1974, 253.
6. R. J. Charles, Studies of the Brittle Behavior of Ceramic Materials, ASD-TR-61-628, 1963, 467.
7. J. Lankford, Jour. Mat. Sci. (in press).
8. J. Lankford, Scripta Met., 11, 1977, 349.
9. M. L. Kronberg, Jour. Am. Cer. Soc., 45, 1962, 274.
10. O. Johari and N. M. Parikh, Frac. Mech. Cer., Vol. 1, ed. R. C. Bradt, D. P. H. Hasselman, and F. F. Lange, Plenum Press, N.Y. 1974, 399.
11. J. M. Samuels; M. R. Hoover, Jr.; L. Tarhay; G. G. Johnson, Jr.; H. A. McKinstry; E. W. White, ibid, 421.
12. P. L. Gutshall and G. E. Gross, Eng. Frac. Mech., 1, 1969, 463.
13. J. B. Wachtman, Jr., and D. G. Lam, Jr., J. Am. Cer. Soc., 42, 1959, 254.